

Electronic Supplementary Information

Covalently hybridized carbon-dots@mesoporous silica nanobeads as a robust and versatile phosphorescent probe for time-resolved biosensing and bioimaging

Zixuan Liao,^{a,b} Yuhui Wang,^{a,b,c,*} Yu Lu,^{a,b} Ruoxi Zeng,^{a,b} Lin Li,^{a,b} Hao Chen,^b Qingwei Song,^b
Kaizhe Wang,^{b,c} Jianping Zheng^{b,c,*}

^a Wenzhou Medical University, Wenzhou 325035, P. R. China.

^b Ningbo Key Laboratory of Biomedical Imaging Probe Materials and Technology, Ningbo Institute of Materials Technology & Engineering, Chinese Academy of Sciences (CAS), Ningbo 315201, P. R. China.

^c Cixi Institute of Biomedical Engineering, Ningbo 315302, P. R. China.

CORRESPONDING AUTHOR. Dr. Y. Wang, Email: wangyuhui@nimte.ac.cn; Prof. J. Zheng, Email: zhengjianping@nimte.ac.cn

Experimental

Preparation of the CDs.

The CDs were prepared by a microwave assisted carbonization manner that reported in our previous work (*Angew. Chem. Int. Ed.* 2018, 57, 6216–6220.). In brief, ethanolamine (4.0 mL) was dissolved in deionized water (16 mL), and 8.0 mL of phosphoric acid was added dropwise while stirring. After stirring for 30 min, the mixture formed was transferred to a 100 mL beaker, and heated in a domestic oven for 4 min (700 W). After being cooled to room temperature, the obtained brownish-yellow gel-like solid was dissolved by adding deionized water (30 mL). The crude product was centrifuged at 10000 rpm for 15 min to remove large particles, and then pH value of the solution was adjusted to neutrality with sodium carbonate. After a filtration against 0.22 μm membrane, the resulting

filtrate was dialyzed via a dialysis membrane (1000 MWCO) for one week. After a freeze-drying, the final product i.e. pale yellow CDs powder was harvested.

Calculation of the CDs loading efficiency.

The loading efficiency of CDs was measured by Uv-vis absorption method. First, a standard fitting curve between varying CDs concentrations and the corresponding absorption values. Subsequently, the absorption of supernatant liquid was measured, and thus, the free CDs in supernatant liquid was calculated through the above standard curve. So, the weight of doping CDs in DMSNs was obtained through a subtraction of free CDs from the primary CDs (500 mg). Finally, the loading efficiency of CDs was calculated via weight ratio.

FA functionalization of the CDs@DMSNs.

The CDs@DMSNs were first functionalized with amino groups by b-PEI coating via electrostatic interaction. In brief, b-PEI (200 mg) was added into of CDs@DMSNs (10 mL, 10 mg/mL) aqueous solution. After stirring for 24 h, the precipitate i.e., amino modified CDs@DMSNs was obtained by centrifugation and washing with ethanol and water. Subsequently, FA was covalently conjugated onto the surface of CDs@DMSNs through amide condensation reaction. Briefly, FA (100 mg) was dissolved in PBS (5 mL, 0.01 M, pH 7.4). Then, EDC (100 mg) and NHS (120 mg) were successively added, then the solution was stirred at room temperature overnight. The CDs@DMSN-NH₂ (10 mL, 10 mg/mL, PBS) dispersion was added to the resulting solution, and continue the reaction for 12 h. The solution is purified by centrifugation (10,000 rpm, 10 min) by washing with PBS, and the final precipitate i.e. CDs@DMSNs-FA was collected and dissolved in PBS buffer.

MCF-7 cell detection using the CDs@DMSNs-FA probe.

A 96-well plate was selected as the phosphorescence detection platform of MCF-7. First, the amino-modified 96-well plate was grafted with FA through amide condensation reaction. In brief, each hole of a 96-well plate was added PBS buffer (100 μ L, pH 6.7, 10 mM) containing EDC (10 μ g/mL), NHS (15 μ g/mL), and FA (10 μ g/mL). After an overnight reaction, the holes were washed with PBST buffer (pH 7.4, 10 mM) for two times. And so, the 96-well plate with FA functionalization was successfully obtained. Meanwhile, MCF-7 cells were cultured for 24 h. After digestion, the cells were resuspended with fresh medium containing the CDs@DMSNs-FA probe (150 μ g/mL) and suspended for 2 h.

Thereafter, the cells were diluted in a gradient according to different cell densities (10^3 , 10^4 , 5×10^4 , 10^5 , 5×10^5 , 10^6 cell/mL), and the corresponding suspensions (100 μ L) were placed in the plate, with each concentration set up in 5 replicate wells. After 1 hour of incubation at 37 °C, the supernatant was aspirated, and the cells were gently washed three times with PBS buffer (pH 7.4, 10 mM). Then, the plate was subjected to a multifunctional microplate detector with the testing mode of time resolution (Excitation: 355 nm, Emission: 530 nm, delay time: 25 μ s).

Cytotoxicity assessment of the CDs@DMSNs.

Cytotoxicity of the CDs@DMSNs was assessed by a standard CCK-8 assay. In simple, three different cell lines i.e. MCF-7, HEK-293, and NIH-3T3 (10,000 cells/200 μ L) were cultured in 96-well plates for 24 h, respectively. The culture medium was then aspirated and replaced with 100 μ L of fresh medium containing different concentrations of CDs@DMSNs, and continued to be cultured for 24 h. After the addition of the CCK-8 staining agent for another 3 h, the corresponding cell viabilities were measured by a microplate reader at the absorbance of 450 nm.

Supplementary Figures

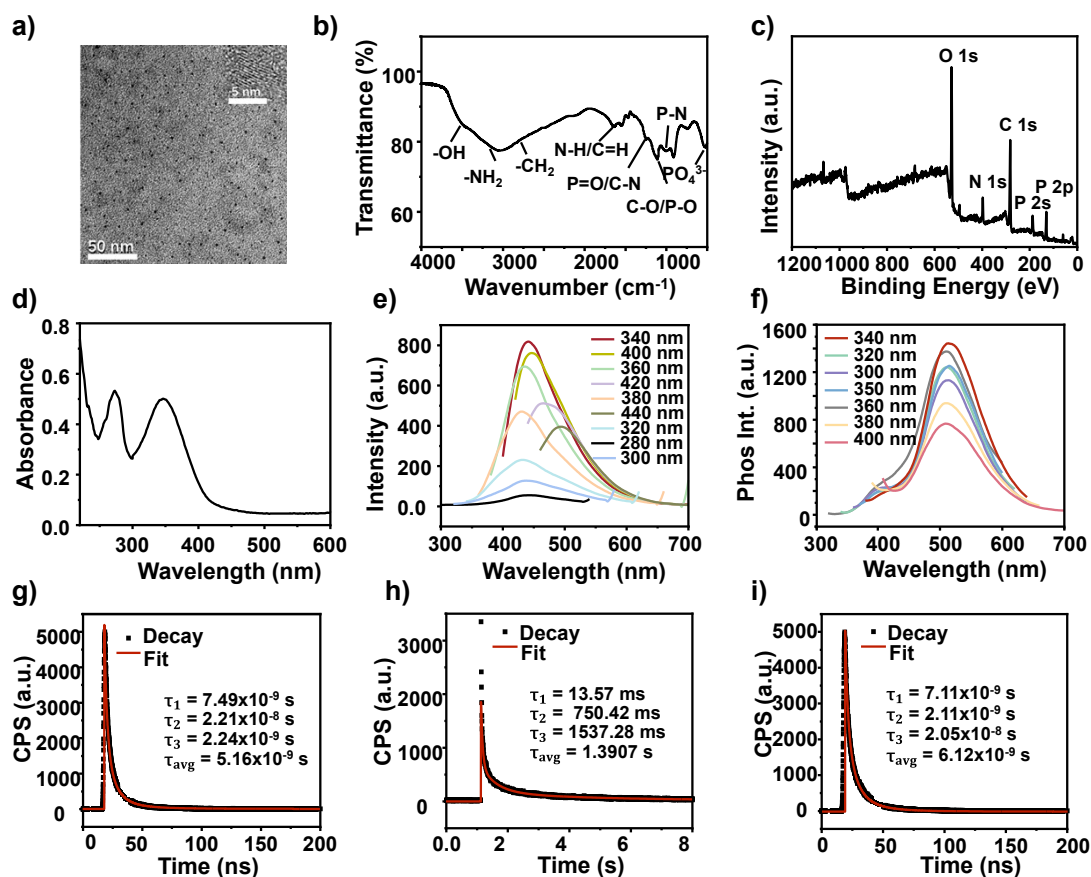


Fig. S1. a) TEM and HR-TEM (inset) images of the CDs. FTIR spectrum (b). XPS spectrum (c) UV-vis absorption spectrum (d). fluorescence emission spectra (e) and solid RTP spectra of the CDs. g) Fluorescence decay curve of the CDs powder ($\lambda_{\text{ex}} = 340 \text{ nm}$, $\lambda_{\text{em}} = 450 \text{ nm}$). h) Phosphorescence decay fitting curve (red line) of the CDs powder under ambient conditions (excitation and emission wavelengths were set at 340 nm and 510 nm, respectively). i) Fluorescence decay spectrum of the CDs aqueous solution ($\lambda_{\text{ex}} = 340 \text{ nm}$, $\lambda_{\text{em}} = 425 \text{ nm}$).

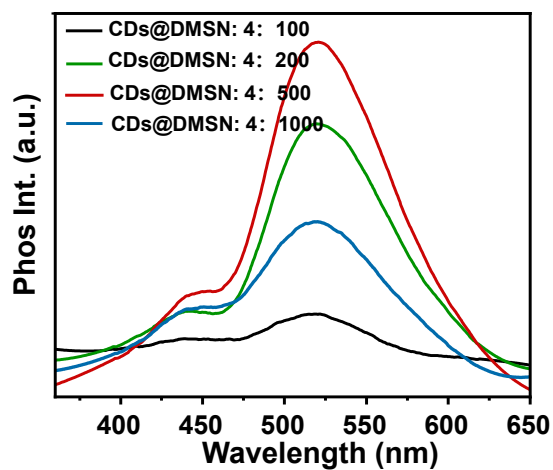


Fig. S2. The afterglow emission spectra of CDs@DMSNs prepared with different ratios of TEOS to CDs by volume (mL) to mass (mg) (i.e. 4:100, 4:200, 4:500, 4:1000, respectively) with the excitation of 365 nm.

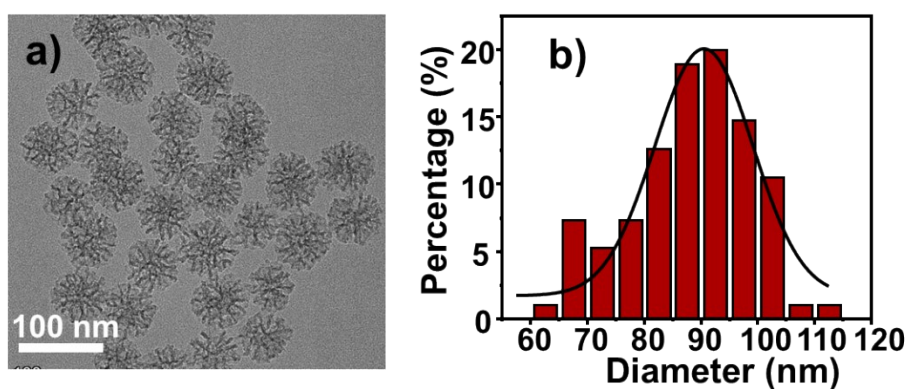


Fig. S3. TEM image (a) and particle size distribution (b) of the DMSNs.

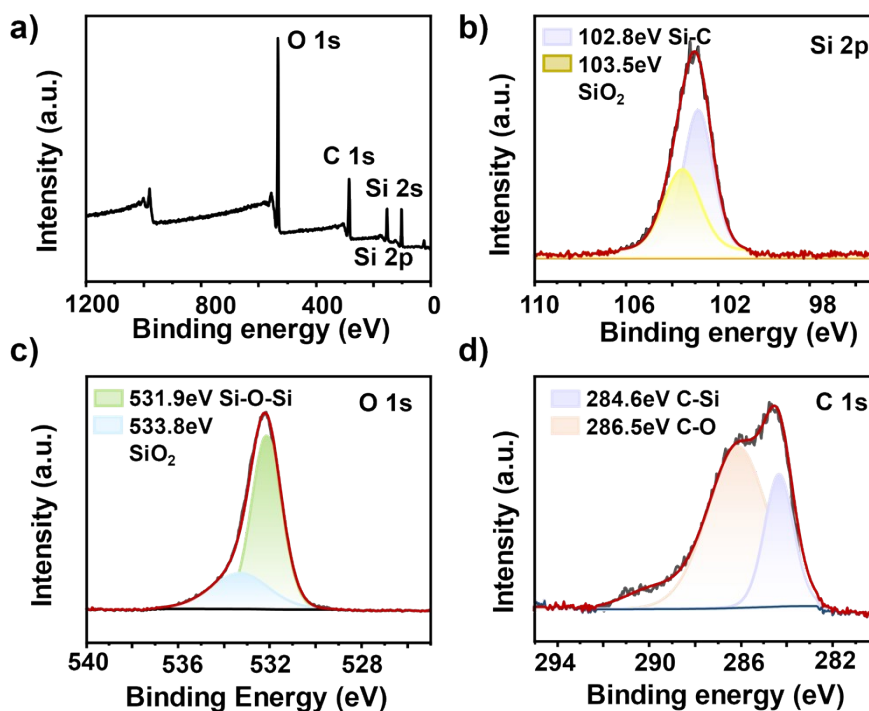


Fig. S4. a) XPS spectrum of the DMSNs. High-resolution XPS spectra of Si 2p (b), O 1s (c), and C 1s (d) of the DMSNs, respectively.

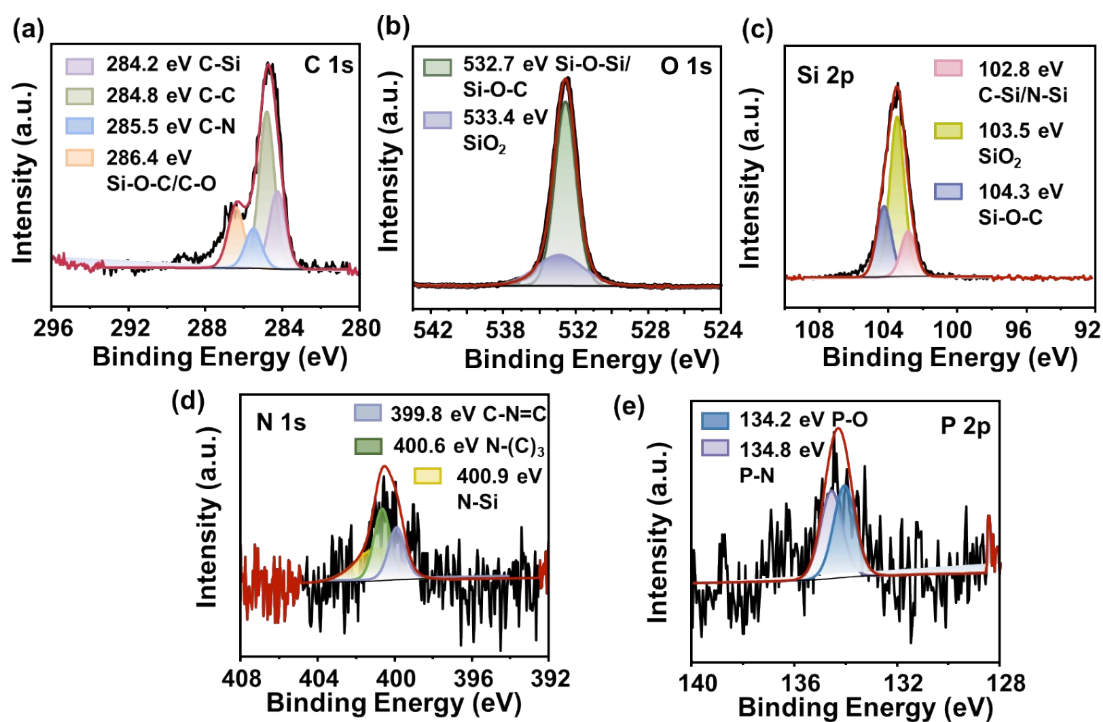


Fig. S5. High-resolution XPS spectra of C 1s (a), O 1s (b), Si 2p (c), N 1s (d), and P 2p (e) of the CDs@DMSNs, respectively.

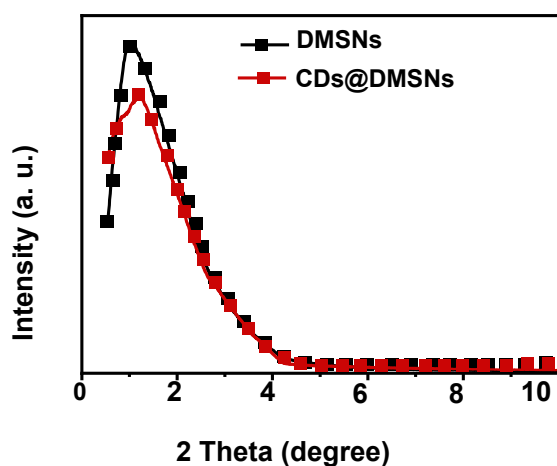


Fig. S6. Small angle XRD of the DMSNs and the CDs@DMSNs nanobeads, respectively.

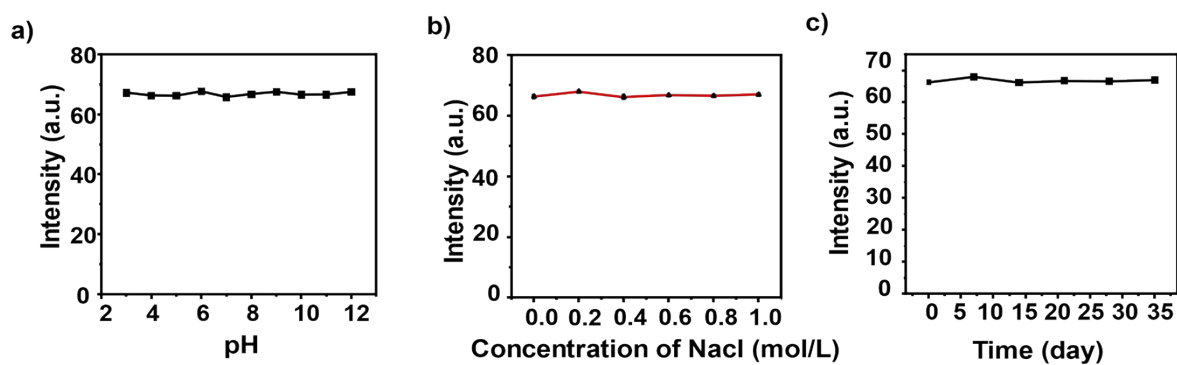


Fig. S7. a) RTP spectra of the aqueous CDs@DMSNs under different pH values. RTP emission intensities of the CDs@DMSNs solution against varying ionic strength (b) and different storage times at ambient conditions (c). The concentration of CDs@DMSNs is 100 $\mu\text{g/mL}$. The excitation ($\lambda_{\text{ex}} = 340 \text{ nm}$) and emission ($\lambda_{\text{em}} = 510 \text{ nm}$) were adopted for RTP quantitative analysis.

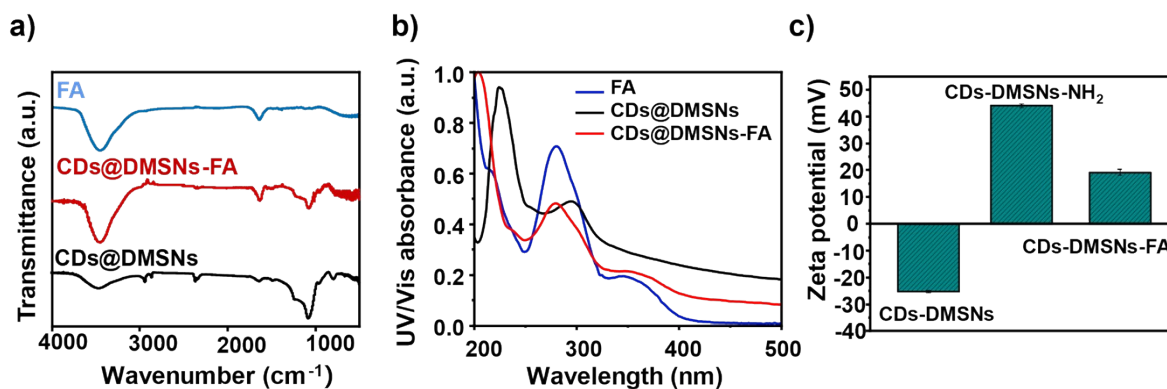


Fig. S8. a) FT-IR spectra of FA, CD@DMSNs, CD@DMSN-FA, respectively. b) UV-vis absorption spectra (black line) of CD@DMSNs, CD@DMSNs-FA (red line), and FA (blue line). c) Zeta potential measurements of CD@DMSNs, CD@DMSNs-NH₂, and CD@DMSNs-FA, respectively.

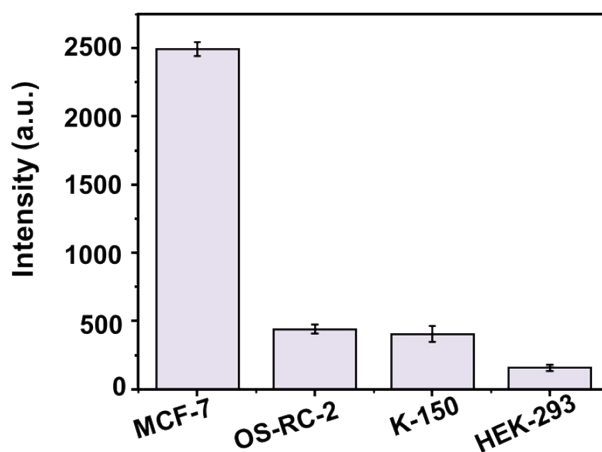


Fig. S9 Quantitative intracellular fluorescence intensities of the CD@DMSNs-FA probe in MCF-7, OS-RC-2, K-150, and HEK-293 cells, respectively.

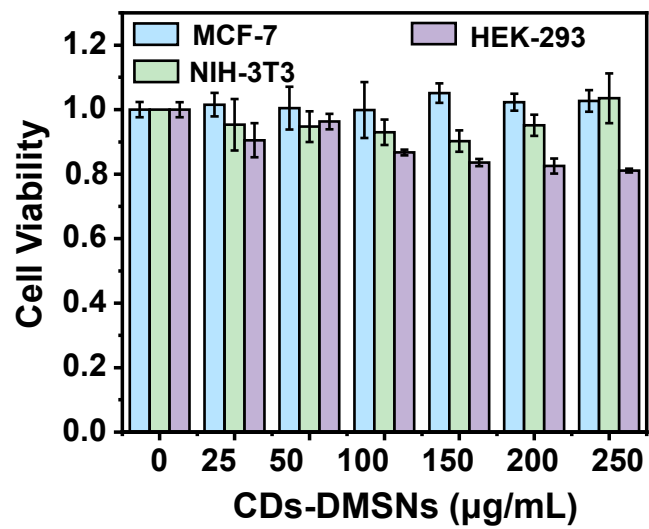


Fig. S10. Cytotoxicity estimation of the CDs@DMSNs using a routine CCK-8 method toward MCF-7, HEK-293 and NIH-3T3 cells.

Table S1. A comparison on the pore structure between DMSNs and CDs@DMSNs.

	BET Surface Area (m^2/g)	Pore Volume (cm^3/g)	Pore Size (nm)
DMSNs	368.3530	1.379221	11.8883
CDs@DMSNs	331.3931	1.126449	10.9119

Table S2. Phosphorescence lifetime fitting results for the CDs@DMSNs measured at different temperatures.

T[K]	τ_1 [s]	B_1 [%]	τ_2 [s]	B_2 [%]	τ_3 [s]	B_3 [%]	τ_{avg} [s]	ϕ
77	0.525	20.55	2.122	76.05	0.054	3.41	2.020	1.39
273.15	0.211	20.46	1.100	75.90	0.015	3.64	1.056	1.21
298.15	0.199	24.90	1.097	70.05	0.019	5.06	1.041	1.097
323.15	0.179	22.84	0.982	72.18	0.013	4.98	0.937	1.051
348.15	0.124	22.84	0.817	71.08	0.010	6.08	0.784	1.083
373.15	0.011	6.60	0.107	25.65	0.707	67.75	0.674	1.138
398.15	0.064	22.35	0.006	10.63	0.468	67.01	0.450	1.107
423.15	0.003	7.18	0.030	24.70	0.277	68.13	0.267	1.075

Table S3. Detailed comparison between CDs@DMSNs and other CDs-based hydrophilic RTP composites.

Materials	Methods	Lifetime (s)	Morphology	Dispersity	Refs
CNDs-RhB@silica	Silica coating	0.91	Uniform	Crosslink and aggregate	1
CDs@nSiO ₂	Surface covalent fixation	0.703	Uniform	Crosslink and aggregate	2
CD-CA	Hydrogen bond fixation	0.687	irregular	Aggregate	3
Melamine-CDs	Hydrogen bond fixation	0.664	Uniform	Crosslink	4
CDs@MP	Inorganic salt melting	1.28	Uniform	Crosslink	5
m-CDs-PVA	Polymer-based hydrogen stabilization	0.456	irregular	Crosslink	6
CDs@DMSNs	covalent	1.195	Uniform	Monodisperse	This work

References

1. Y.C. Liang, Q. Cao, K.K. Liu, X.Y. Peng, L.Z. Sui, S.P. Wang, S.Y. Song, X.Y. Wu, W.B. Zhao, Y. Deng, Q. Lou, L. Dong, and C.X. Shan, *ACS Nano*. **2021**, *15*, 16242-16254.
2. K. Jiang, Y.H. Wang, C.Z. Cai, and H.W. Lin, *Chem. Mater.* **2017**, *29*, 4886-4873.
3. Q.J. Li, M. Zhou, M.Y. Yang, Q.F. Yang, Z.X. Zhang, and J. Shi, *Nat. Commun.* **2018**, *9*, 734.
4. Y.F. Gao, H.L. Zhang, Y. Jiao, W.J. Lu, Y. Liu, H. Han, X.J. Gong, S.M. Shuang, and C. Dong, *Chem. Mater.* **2019**, *31*, 7979-7986.
5. C. Wang, Y.Y. Chen, Y.L. Xu, G.X. Ran, Y.M. He, and Q.J. Song, *ACS Appl. Mater. Interfaces*. **2020**, *12*, 10791-10800.
6. X.Y. Wu, C.H. Ma, J.C. Liu, Y.S. Liu, S. Luo, M.C. Xu, P. Wu, W. Li, and S.X. Liu, *ACS Sustainable Chem. Eng.* **2019**, *7*, 18801-18809.